Comparative results on the total ozone content reconstructed from data of the UV spectrophotometer with a narrow-field-of-view receiving antenna and an M-124 ozonometer

M.V. Grishaev, V.V. Zuev, I.V. Ptashnik, and S.V. Smirnov

Institute of Atmospheric Optics,
Siberian Branch of the Russian Academy of Sciences, Tomsk
Received December 30, 1998

The use of a UV spectrophotometer with a narrow field of view is considered as applied to reconstruction of the total ozone content from measurement results on sky spectral brightness in zenith. The instrumentation is briefly described, along with techniques for measurement and processing of experimental data. The results of reconstruction of the total ozone content are compared with the data of an l −124 ozonometer.

Introduction

The problem of atmospheric ozone is among the major research areas at Siberian Lidar Station of the Institute of Atmospheric Optics SB RAS. Being a strong absorber of the UV radiation, ozone plays a very important part in the atmospheric radiative, physical, and chemical processes, governs the thermal conditions in the stratosphere, and protects the Earth's surface against the biologically active hard UV radiation. Ozone depletion and formation of ozone anomalies (ozone holes) over the Antarctic, Europe, and Siberia have shown the necessity of monitoring the ozone layer on the global scale. Ground-based ozonometric stations typically employ Dobson and Brewer ozonometers, or M-124 filter ozonometer (over the territory of Russia). At the same time, many research groups currently utilize passive methods of atmospheric sounding.[1–4] These methods are less expensive and allow observations in an unattended mode.

This paper discusses the possibility of using a high-sensitive spectrophotometer with an optical receiving antenna for measurements of the spectral brightness of the sky in zenith. The optical antenna to be used should have a narrow field of view and high spectral resolution in the wavelength range from 280 to 340 nm. This allows solution of the equation of transfer with regard for only single scattering. The results on the total ozone content (TOC) obtained are presented in comparison with the data obtained with an l -124 ozonometer at Siberian Lidar Station of the Institute of Atmospheric Optics SB RAS.

Instrumentation and measurement technique

Block diagram of the spectrophotometer is shown in Fig. 1. The solar radiation scattered in zenith is collected by a Cassegrainian telescope with the primary mirror diameter of 30 cm. Then the radiation is directed with a beam-folding mirror *2* to the entrance slit *4* of an MDR−23 monochromator. Filter *3* provides for transmission in the region from 250 to 360 nm; it is needed to eliminate higher orders of diffraction in the monochromator. Spectra are recorded in the region from 260 to 340 nm; spectral resolution is 0.2 nm; the scanning step is 0.01 nm. The signal is detected with a FEU−71 photomultiplier tube operated in a photon counting mode. Single-electron pulses are amplified with a broadband amplifier up to the amplitude of 0.5 V. An amplitude discriminator converts the amplified output pulses exceeding the threshold value into a standard signal for actuating an 8-bit binary counter. The amplitude selection of pulses allows an increase in the signal-to-noise ratio due to reduction of noise.

The counter of single-electron pulses comprises an 8-bit binary counter and two timers of a single-chip microcontroller. The first timer measures the time of accumulation, while the second one counts overflows of the 8-bit binary counter. As the interval of accumulation completes, the microcontroller sends two bytes of the number of overflows (one counting cycle corresponds to 256 single-electron pulses) and one byte of the number of pulses counted by the 8-bit counter. Then the counter resets and sends the ready command to start a new accumulation cycle. An 89C51 Intel microcontroller controls the timers, high-voltage power supply, the stepper motor of the monochromator sine mechanism, and the gate. It is also responsible for transmission and reception of commands and data. The microcontroller operates under a special program stored in its PROM. The controlling computer sends the commands to set a monochromator grating at its initial point, turns on the high-voltage power supply, turns off the gate, and measures the dark current. Then the computer turns the controller into the measurement mode and acquires the data. After completion of measurements, the data are stored as a file onto a hard disk. Then these files are used as input information for the program of TOC calculation.

0235-6880/99/05 418-04 $02.00

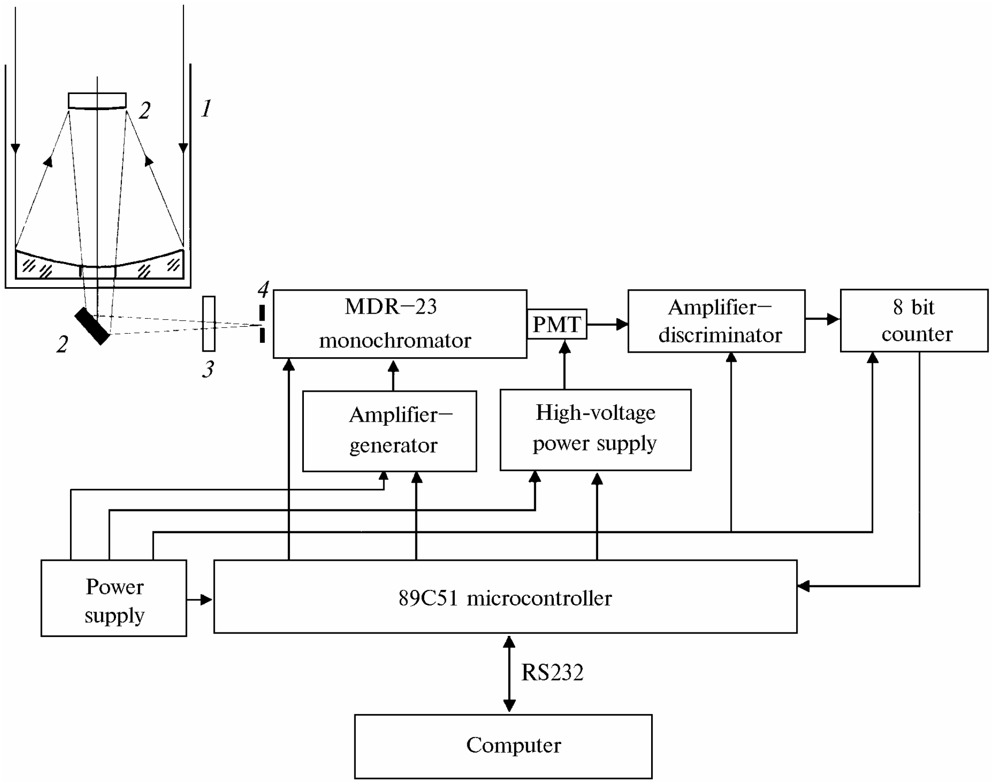

Fig. 1. Block diagram of the spectrophotometer: telescope (*1*); beam-folding mirror (*2*); optical filter (*3*); monochromator entrance slit (*4*).

Technique of total ozone content reconstruction

Determination of TOC is based on solution of the equation of transfer in the single-scattering approximation. The solar radiation scattered in zenith and recorded with the spectrophotometer can be described by the following equation:

$$I(\lambda) = S_0(\lambda)\ C(\lambda) \int\limits_{\Delta\lambda} \mathrm{d}\lambda'\ h(\lambda - \lambda') \int\limits_0^H \mathrm{d}(\lambda', \theta, z) \times$$

$$\times \exp\left[-\int\limits_0^Z \alpha_\Sigma(\lambda, z')\mathrm{d}z' - \int\limits_Z^H B(z, z', \theta)\, \alpha_\Sigma(\lambda, z')\mathrm{d}z' \right] \mathrm{d}z; \quad (1)$$

$$\alpha_\Sigma(\lambda, z) = k_\mathrm{g}(\lambda, z)\ \rho_\mathrm{g}(z) + \alpha_\mathrm{a}(\lambda, z) +$$

$$+ \alpha_\mathrm{m}(\lambda, z) + \sum_{i\neq \mathrm{g}} k_i(\lambda, z)\ \rho_i(z);$$

$$d(\lambda, \theta, z) = \alpha'_\mathrm{a}(\lambda, z)\ g_\mathrm{a}(\theta) + \alpha_\mathrm{m}(\lambda, z)\ g_\mathrm{m}(\theta);$$

$$B(z, z', \theta) = 1 \Big/ \sqrt{1 - \left(\frac{R + z}{R + z'}\frac{n(z)}{n(z')} \sin\theta\right)^2},$$

$S_0(\lambda)$ is the solar constant; $C(\lambda)$ is the instrumental function including the field-of-view angle of the receiving system, the area of the receiving mirror, the transmittance of optical elements, the quantum efficiency of a PMT, and other parameters; θ is the solar zenith angle; $d(\lambda, \theta, z)$ is the total coefficient of aerosol and molecular scattering at an angle θ from the initial direction at the altitude z above the sea level; $k_\mathrm{g}(\lambda, z)$ and $k_i(\lambda, z)$ are the altitude profiles of the absorption coefficients of the gas under study and the ith foreign gaseous constituent; H is the effective top of the atmosphere; $\rho_\mathrm{g}(z)$ and $\rho_i(z)$ are the altitude profiles of the density of a gas under study and foreign gases; $\alpha'_\mathrm{a}(\lambda, z)$ and $\alpha_\mathrm{m}(\lambda, z)$ are the profiles of the aerosol and molecular scattering coefficients; $g_\mathrm{a}(\theta)$ and $g_\mathrm{m}(\theta)$ are the corresponding scattering phase functions; $\alpha_\mathrm{a}(\lambda, z)$ is the aerosol extinction coefficient; R is the Earth's radius; $h(\lambda - \lambda')$ is the instrumental function of a device. Assuming that optical characteristics change negligibly within $\Delta\lambda = 0.1$ nm (Ref. 5), from here on we ignore the influence of the instrumental function on the measurement results.

Then, introducing the total content of a gas as

$$X = \int\limits_0^H \rho_\mathrm{g}(z)\ \mathrm{d}z\ ,$$

and assuming k_g to be height-independent, i.e., replacing it with the mean effective value

$$k_g(\lambda, z) = k_g(\lambda) = \frac{\int k_g(\lambda, z)\, \rho_g(z)\, dz}{\int \rho_g(z)\, dz},$$

and taking logarithm of Eq. (1), we obtain

$$X = \frac{1}{k_g(\lambda)} \left\{ \ln \left[\frac{S_0(\lambda)\, C(\lambda)}{I(\lambda)} \right] - [\tau_a(\lambda) + \tau_m(\lambda) + \tau_f(\lambda)] + \right.$$
$$\left. + \ln\, [JS(\lambda, \theta)] \right\};$$

$$JS(\lambda, \theta) = \int_0^H d(\lambda, \theta, z) \times$$
$$\times \exp \left\{ \int_z^H \alpha_\Sigma(\lambda, z')\, [1 - B(z, z', \theta)] dz' \right\} dz.$$

Here

$$\tau_a(\lambda) = \int_0^H \alpha_a(\lambda, z)\, dz,$$

$$\tau_m(\lambda) = \int_0^H \alpha_m(\lambda, z)\, dz, \quad \tau_f(\lambda) = \int_0^H \sum_{i \neq g} k_i(\lambda, z)\, \rho_i(z)\, dz$$

are the vertical optical thickness due to aerosol extinction, molecular scattering, and light absorption by foreign gases, respectively.

Using the model ozone profiles k_g (Ref. 6), literature data on S_0 (Ref. 8), and models of α_a, α_m, α_f, g_a, and g_m (Ref. 7), we can find the total ozone content from the spectrophotometer data. Details of calculation technique and estimates of an error can be found in Ref. 9.

Experimental results compared with data of an M-124 ozonometer

Figure 2 shows the TOC values reconstructed from the sky spectral brightness measurements with an M-124 ozonometer and the spectrophotometer. The data obtained for three periods are compared in this figure. The first period (July 23–30) is associated with tuning of the instrumentation and characterized by unstable reconstruction of TOC. The second period starts on August 3. This day was characterized by a fine weather. However, two days later some clouds appeared on the sky. On August 17–19 short-time rains fell, which broke continuity of the observation series. The third period (August 19–30) is characterized by sharp changes in TOC. The total number of the days of observation was 32. From Fig. 2 it is seen that both of the devices similarly follow up the tendencies in TOC variability and give close values. The correlation coefficient calculated from this data array is 0.769. Figure 3 shows the difference between the TOC values obtained with both of the devices. As seen, almost all points are within ±5% interval. It should also be noted that the days with maximum discrepancy were characterized by the presence of broken clouds, which contributed significantly to fluctuations of the measured signals.

Thus, the comparative analysis shows that the developed spectrophotometer with the narrow-field-of-view receiving antenna provides for TOC measurements with a sufficient accuracy. The performance characteristics of the spectrophotometer can be further improved by allowing for correlation between signal modulation and cloudiness and by increasing the sensitivity at the wavelengths shorter than 280 nm.

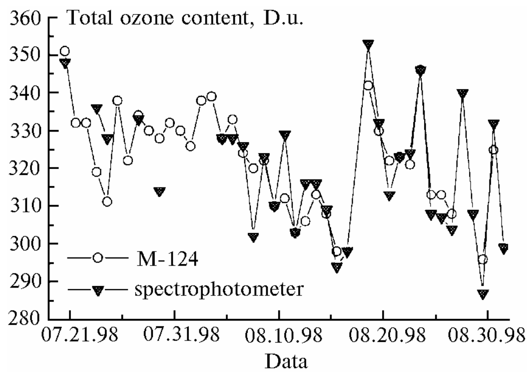

Fig. 2. TOC values measured with the UV spectrophotometer and an M-124 ozonometer.

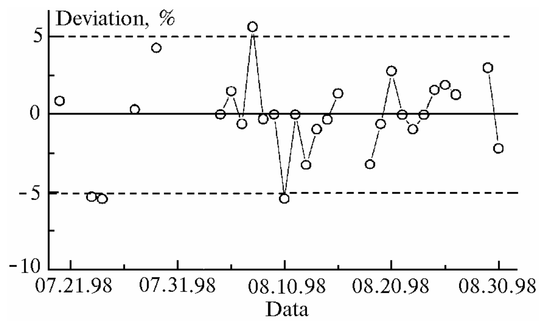

Fig. 3. Discrepancy between the TOC values estimated from data of the UV spectrophotometer and an M-124 ozonometer.

Acknowledgments

This work was supported in part by the Russian Foundation for Basic Research (Project No. 96–05–64282).

References

1. S.P. Perov and A.Kh. Khrgian, *Modern Problems of Atmospheric Ozone* (Gidrometeoizdat, Leningrad, 1980), 288 pp.

2. A.M. Shalamyanski and K.I. Romashkina, Trudy Gl. Geofiz. Obs., Issue 445, 116–123 (1980).

3. G.P. Gushchin and S.A. Sokolenko, Trudy Gl. Geofiz. Obs., Issue 472, 31–35 (1984).

4. K.I. Romashkina, Trudy Gl. Geofiz. Obs., Issue 472, 100–107 (1980).

5. L.G. Bol'shakova, Izv. Akad. Nauk SSSR, Ser. Fiz. Atmos. Okeana **12**, No. 9, 969–978 (1976).

6. I.I. Ippolitov, V.S. Komarov, and A.A. Mitsel', in: *Spectroscopic Methods of Atmospheric Sounding* (Nauka, Novosibirsk, 1985), pp. 4–44.
7. G.M. Krekov and R.F. Rakhimov, *Optical Model of Atmospheric Aerosol* (Publishing House of the Tomsk Affiliate of the Siberian Branch of the USSR Academy of Sciences, Tomsk, 1986), 294 pp.
8. J.C. Arvesen, R.N. Griffin, and B.D Pearson, Appl. Opt. **8**, No. 11, 2215–2232 (1969).
9. S.I. Dolgii, V.V. Zuev, V.N. Marichev, A.A. Mitsel', I.V. Ptashnik, and V.P. Sorokin, Atmos. Oceanic Opt. **9**, No. 5, 384–395 (1996).